Journal of Structural Geology, Vol. 13, No. 3, pp. 261 to 274, 1991
Printed in Great Britain

0191-8141/91 $03.00+0.00

Nomenclature and geometric classification of cleavage-transected folds

T. E. JOHNSON

Department of Earth Sciences, University of Cambridge, Downing Street, Cambridge CB2 3EQ, U.K.

(*Received* 3 *November* 1989; *accepted in revised form* 18 *June* 1990)

Abstract—Terms and measures for describing real and theoretical three-dimensional cleavage-transected folds are reviewed and clarified. The geometrically possible range of cleavage-transected folds is explored. Reappraisal and extension of published measures allows study of geologically realistic asymmetrical folds. Scale-related description of cleavages and associated folds is formalized and sampling problems discussed. The plot comparing axial- with profile-plane fold transection by cleavage is used to classify transected folds in a geometrical manner. It helps reveal the constitutive geometry of cleavage-transected folds and should help identify the most actively growing fold order during a cleavage-forming episode. Plotted examples from Welsh asymmetric cleavage-transected folds of Acadian age show complex transection geometries.

INTRODUCTION

THE AIM of this paper is to clarify and illustrate the terms and geometric measures used to describe cleavage-transected folds (CTFs). The phrase *cleavage-transected fold* is used throughout in its widest sense (Powell 1974) to include folds whose cleavage refracts, fans or apparently 'overprints' folds as well as cuts across fold axes, and where there is a lack of evidence suggesting that more than one deformational episode is responsible for folding and cleavage.

The proposed nomenclature aims to be descriptive. It is based on both previously defined and newly defined measures. Practical and theoretical measures used by previous workers are discussed. Cleaved folds of Acadian age from mid-Wales are used as examples to illustrate these geometrical concepts. Throughout these discussions it is assumed that, excepting the compactional fabric, a *single* upright tectonic cleavage affects folds (but see Williams 1985, Tobisch & Paterson 1988).

Folds with an associated cleavage which is non-axial planar in some respect have been observed since cleavage was first distinguished from sedimentary bedding (Sedgwick 1835). Indeed, mesoscopic folds parasitic on macroscopic folds were described by later workers as pre-tectonic if they were visibly transected. Refraction (Sorby 1853) and fanning (Sedgwick 1835) of cleavages were also observed. This was called "cleavage folding" by some authors (Ward 1876). Subsequently, most observers of syntectonic folds and foliations found that axial planes and cleavages were essentially parallel, or at least that refraction and fanning greatly exceeded any non-parallelism of cleavage to fold axes. A persistent obliquity between fold axes or hinges and associated cleavages has been recognized by an increasing number of workers from the 1950s onward.

FOLD GEOMETRICAL FRAMEWORK

The main geometric descriptors of natural multilayer folds must first be reviewed. These comprise: (a) those relating to layer-boundary curvature, such as inflection and hinge points, and the lines and surfaces defined by the loci of these points (e.g. fold axial surfaces—see also Twiss 1988); (b) those dependent upon layer-boundary attitude, such as crestal and trough points, lines and surfaces; (c) those describing variations in shape and thickness of the folded layers themselves, such as dip isogons (Elliot 1965) and isogon angles (ϕ of Hudleston 1973, p. 7), and various thickness parameters (e.g. the terms T_α, t_α of Ramsay 1967, pp. 359–362); and (d) measures of the geometry of foliations compared with the geometry of the boundaries of folded layers, such as β (Treagus 1982).

Further imaginary planes (or surfaces) are necessary for the description of cleavage-transected fold geometry. The surface perpendicular to the axial surface and containing the fold axis (and sometimes the hinge) can be called the *hinge-tangential surface/plane* (Fig. 1). The surface containing the fold axis—and generally the hinge—and bisecting the fold limbs is the *limb-bisector surface* (Fig. 2). Both of these planes have traces in the profile plane (Fig. 2). A fold axial surface trace (hinge surface trace of some authors) is difficult to define in profile sections except where it is directly measurable. This is because information on layer thickness variations around folds is usually limited in areas of poor outcrop.

The symmetry of layer boundaries and layer thickness variation can be described in terms of the symmetry classes. Folds possessing orthorhombic symmetry are symmetrical about an axial plane which is coincident with a limb-bisector plane. In this special case the attitude of the fold axial plane/limb-bisector plane can be determined using various methods. (a) The great circle containing the π-axis and the pole to bedding observed to lie on the fold hinge is the fold axial plane (assuming coincidence of the hinge and axial plane traces in the fold profile). This method should be avoided if the folds are upright because of large measurement errors on gently dipping surfaces (Woodcock 1976). (b) The fold axial plane coincides with the plane containing the π-axis and the bisector of the angle between the bedding poles at fold inflection points on

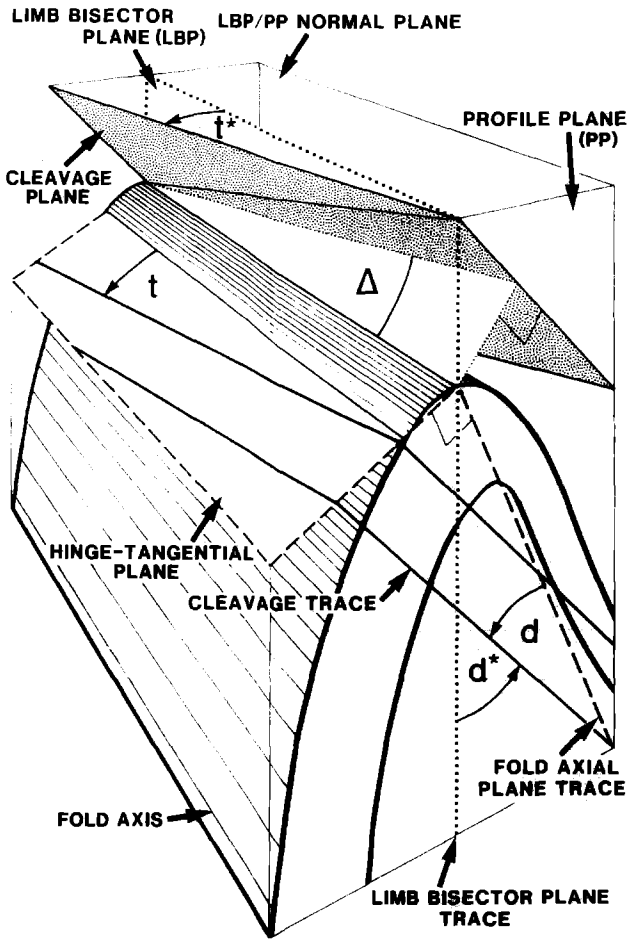

Fig. 1. Asymmetric, upward-facing fold with non-coincident fold axial plane and limb-bisector plane showing the two sets of profile- and 'hinge plane'-transection measures. Measures d and t are found if the fold axial plane is used, whereas d^* and t^* relate to use of the limb-bisector plane. Measure Δ remains of constant absolute magnitude regardless of which plane is used.

the π-circle (assuming the axial plane attitude is known approximately). Alternatively, the vector means of bedding-pole clusters may be used instead of inflection point bedding-poles. This is only valid if fold limb planarity is assumed (i.e. shape parameter—k of Woodcock 1977—is greater than 1 for limb-separated bedding-pole data). (c) The plane containing the intersection of the bulk mean cleavage plane with the profile plane and the π-axis will coincide with the fold axial plane/limb-bisector plane in the special case of non-fanning/non-refracting (bulk) cleavage. Local cleavage orientation at the hinge can be used instead of bulk mean cleavage (Gray 1981), but local cleavage may itself be non-axial planar. (d) The fold axial plane may be found by connecting the centres of ellipses drawn tangential to several folded surfaces in their hinge-zones (Stauffer 1973). This technique may also be applied to asymmetric cylindrical folds.

Asymmetric cylindrical folds may locally approximate monoclinic symmetry (Fig. 2). This means there is no symmetry plane containing the fold axis (the only symmetry plane is the fold profile). Such folds possessing non-planar axial surfaces may approximate monoclinic symmetry in small volumes of affected rock. This will be the case if the axial surfaces are cylindrically curved with generators parallel to fold axes (Wilson 1967). In profile, axial surface traces (joining hinge points on successive layer boundaries) will not coincide with the limb-bisector surface traces (fig. 5 in Hudleston 1973). Generally, this is because the fold limbs have been differentially thinned. Asymmetric folds may have fold axial surface traces which are 'rotated' towards parallelism with the relatively thinned limb. The angle between the limb-bisector surface trace and fold axial surface trace in the profile (β of Hudleston 1973) will vary with the degree of limb thinning or thickening. If a fault-propagation fold model is assumed, then β will vary with dip of the axial surface, displacement on the driving fault, width of deforming zone and layer thickness (Fig. 3). Pre-tectonic inhomogeneities and variations in layer viscosities in a multilayer sequence are likely to result in differential limb thinning. Differential sampling of fold limbs will exert a strong control on the computed limb-bisector surface. Layers of different viscosity should be distinguished so that potential differences in attitude of limb-bisector surface/fold axial surface, and therefore β, can be detected. Further complication is caused by offset of the hinge line from the plane perpendicular to limb-bisector and profile planes and tangential to the folded layer boundary (fig. 14 of Twiss 1988).

Asymmetric non-cylindrical folds possess triclinic symmetry. This results in non-parallelism of the limb-bisector surface and fold axial surface. Such folds do not possess fold axes with which cleavage attitude could be compared. However, on a macroscopic scale the symmetry may be approximately monoclinic (and cylindroidal, Roberts 1982), allowing definition of transection parameters. Also, on a mesoscopic scale parasitic folds

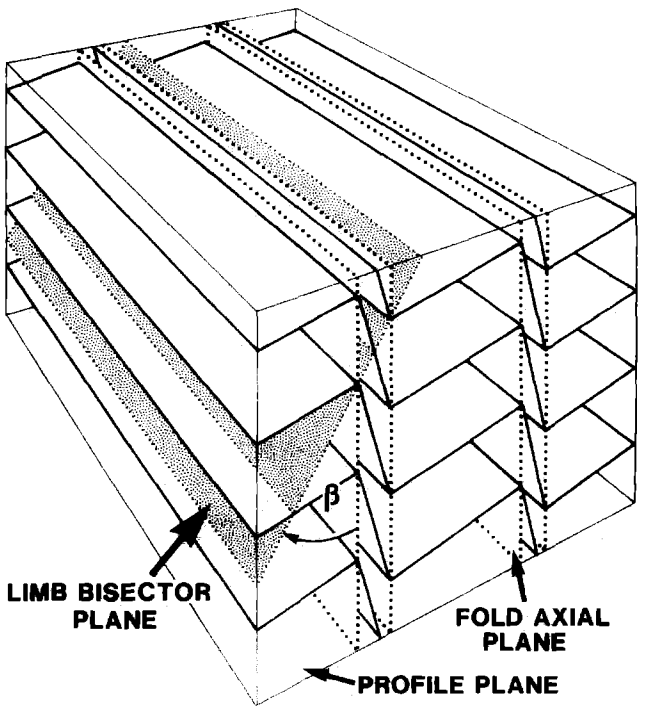

Fig. 2. Angular asymmetric folds showing non-coincidence of vertical fold axial planes with dipping limb-bisector planes. The angle between these planes measured in the profile plane is β (Hudleston 1973).

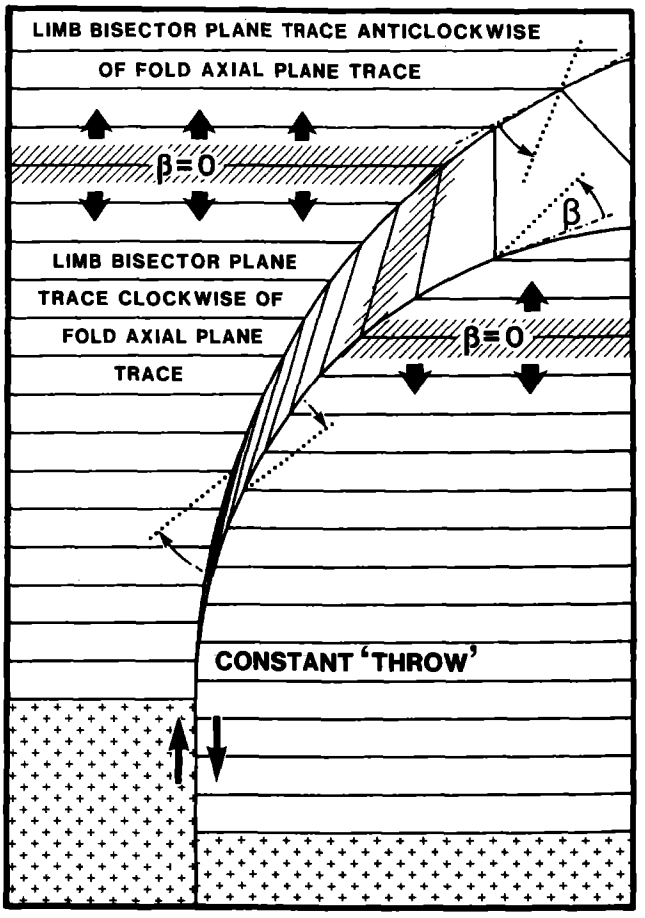

Fig. 3. Fault propagation fold model in which a vertical basement dip-slip fault has a throw of three units. The deforming cover (with constant bed thickness) maintains the same vertical displacement by asymmetric folding in an upward-widening zone. Near to the basement, steep limbs are highly attenuated in response to large simple-shear strains. Here, limb bisector plane traces are clockwise (in this view) of fold axial plane traces. The deforming zone will tend to widen and/or decrease in dip towards the situation in which original bed thickness is preserved while maintaining vertical displacement. This is likely to be the most energetically efficient means of accommodating the displacement. When this situation is reached the limb-bisector and fold axial plane traces are coincident. The situation shown above this, where the limb bisector plane trace is anticlockwise of the fold axial plane trace, is unlikely to occur because of the volume increase needed in the short limb. Therefore the zone is likely to maintain the width and dip seen at $\beta = 0$.

may possess more or less conical form. Symmetrical elliptical conical folds (Stauffer 1963) have cone axes and coincident axial and limb-bisector planes with which cleavage orientation can be compared. Asymmetric elliptical conical folds are probably common in deformed terrains. Cone axes, hinges and axial surfaces may be present but the complex nature of their geometry makes comparison with cleavage planes difficult and beyond the scope of this paper.

DESCRIPTION OF CLEAVAGE-TRANSECTED FOLDS

The first formalized description of transected folds was by Borradaile (1978, p. 482), who defined delta (Δ) as "the dihedral (*sic*) angle between the cleavage plane and the fold axis". A dihedral angle is the smallest angle measured between two planes, not between a plane and a line (Considne 1976). However, Borradaile clarified this by describing Δ as the "angular discrepancy between the fold-axis direction and its projection on the XY plane" (of the strain ellipsoid) and by showing Δ measured in the plane containing the cleavage-normal and fold axis (Borradaile 1978, p. 483 and fig. 1). Borradaile realized that a second angle was needed to describe the transection geometry fully. Therefore, d was defined as the angle between the axial plane trace and the cleavage trace in the fold profile. A further angle, t, is here defined as the inter-trace angle between the axial plane and cleavage in the hinge-tangential plane (Fig. 1).

Because the fold axial plane trace in the profile plane cannot be accurately determined without much layer-thickness variation data, d cannot normally be detected directly. An alternative is to measure the angle between the trace of the limb-bisector plane and the trace of the cleavage in the profile plane, d^* (Fig. 4). The trace of the limb-bisector plane in the profile can be estimated using the methods outlined above. The orthogonal correlative of d^* in the limb-bisector and profile-normal plane is t^* (Fig. 1, this plane contains the "quadrilateral tangent" of Twiss 1988). Notwithstanding the probable variations in β, the estimated attitude of the limb-bisector plane trace can be used as a datum to allow measurement of the relative changes in d^* with respect to Δ. The value of Δ is independent of d/d^* since it is measured relative to the fold axis. Variations in d^* do not necessarily reflect changes in the absolute magnitude of profile transection, since a component of β variation or limb-bisector surface curvature may occur. However, the variation in cleavage refraction angle is likely to exceed β by an order of magnitude at mesoscopic scale. Construction of cross-sections using the isogon reconstruction method (Ramsay & Huber 1987) should indicate the likely range of β, and thus the significance that can be attached to d^* variations in the study area. Given these limitations, the method does allow determination of the relative magnitude and sense of profile-transection compared with axial-transection within a fold at mesoscopic scale.

It is proposed that the term *hinge-(cleavage-) transection* be restricted to direct observations of that phenomenon whereas *axial-(cleavage-)transection* be used to denote non-zero t and Δ-type relationships. This allows for the possibility of triclinic fold symmetry resulting in non-parallelism of hinges and fold axes (see below). *Profile-transection* refers to d-type cleavage-transective geometries whilst *apparent profile transection* might be used for d^*-type transecting relationships. The term *'cleavage-transected fold'* (CTF) should be applied to folds showing hinge and/or axial transection by a mean or bulk cleavage. It should only be applied if there is evidence that folds and cleavage formed during the same progressive deformational episode (in the sense of Powell 1974 and Borradaile 1978). The sense (and sign) of axial- and profile-transection

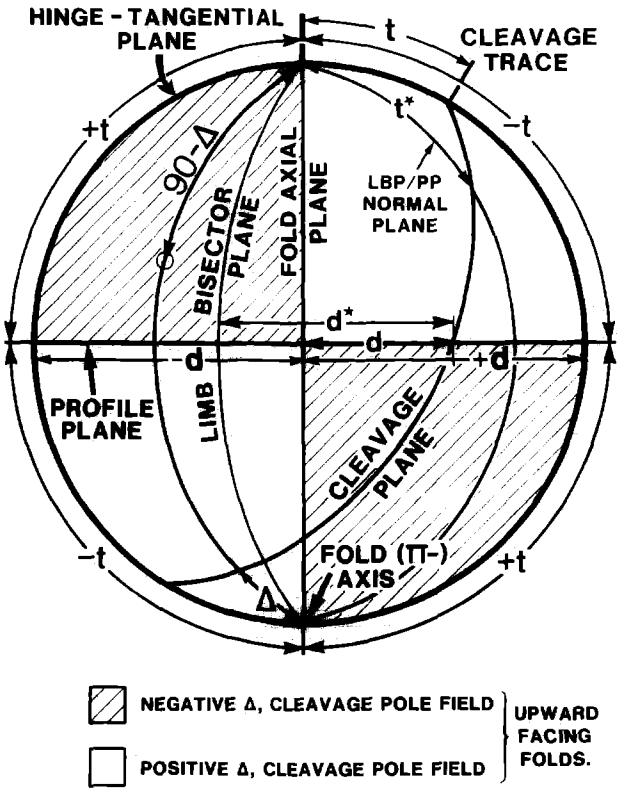

Fig. 4. Lower-hemisphere equal-area projection showing main cleavage-transected fold measures for a theoretical fold. The sense of fold transection can be determined using the convention that clockwise 'rotations' are deemed negative and anticlockwise, positive. Ideally, signs should be determined in the framework of the fold axis/axial plane rather than the limb-bisector plane. The hinge-tangential plane of the fold should be 'viewed', away from the facing direction, along the profile plane–fold axial plane intersection. Using the fold axis as 'northward' datum, if the cleavage trace in the hinge-tangential plane falls in the NE–SW sectors then 'clockwise' fold axial transection by cleavage is indicated. In this case cleavage poles fall in the NW–SE sectors. To determine the sense of profile-transection, the fold profile must be viewed (along the fold axis) in a consistent direction. In this view the fold axial plane trace is used as a datum with the facing direction pointing 'northwards'. The cleavage is then said to be anticlockwise profile-transecting if its trace lies in the NW–SE sectors. For instance, in Fig. 1 the cleavage is anticlockwise axial-transective ($+t/+\Delta$) and anticlockwise profile-transective ($+d$). 'LBP' is limb-bisector plane, 'PP' is profile plane. Also see Fig. 5.

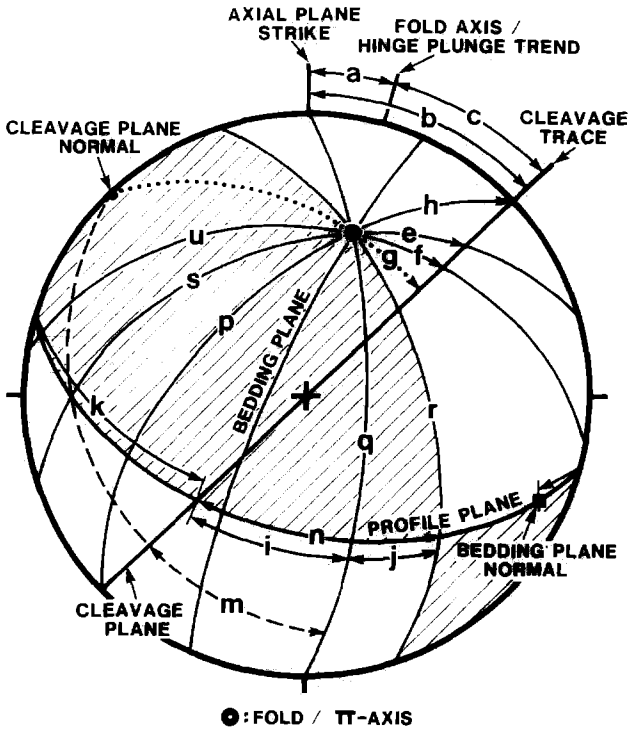

Fig. 5. Lower-hemisphere equal-area projection of a theoretical plunging, inclined and upward-facing fold showing cleavage-transected fold measures used by various authors (see text). Labelled geometric features not in the main text are: a, axial plane strike with respect to fold axis trend; e, t; g, Δ (Borradaile 1978); h, t^*; i, d; j, β (Hudleston 1973); n, d^*; p, plane perpendicular to limb-bisector plane and profile plane; q, axial plane; r, limb-bisector plane; s, hinge-tangential plane; u, fold enveloping plane or median plane. Sign conventions are shown using the limb-bisector plane instead of the fold axial plane. If β is non-zero then $t \neq t^*$ and $d \neq d^*$ but Δ is unchanged in absolute magnitude. The signs of d^* and t^* are determined using the limb-bisector and profile-normal plane and limb-bisector plane as datums (see Fig. 4). The sign changeover of Δ will be shifted by β degrees so that the limb-bisector plane is the new separator between clockwise and anticlockwise axially-transective cleavages. Cleavages which are highly profile-transective, whose poles fall between the limb-bisector plane (r) and fold axial plane (q) will have signs of Δ and d^* that will both change because of the use of the limb-bisector plane (see Fig. 14). Note that the example bedding plane shown has a relationship with the cleavage suggesting downward-facing.

should be determined using the conventions set out in Figs. 4 and 5.

PUBLISHED TERMINOLOGY OF CLEAVAGE-TRANSECTED FOLDS

Practical measurement of geometric elements of cleavage transected folds

Apparent axial-transection of folds by cleavage has been recognized as an angular difference (ϕ) between axial surface trace and cleavage trace in map view or the horizontal plane (Price 1962, Evans 1963, Moseley 1968, p. 83, Wickham 1972, fig.32, Stringer 1975, Davies & Cave 1976, Bell 1978, Anderson & Cameron 1979, Phillips *et al.* 1979, Sanderson *et al.* 1980, Takizawa 1981, Geiser & Engelder 1983, James 1986, p. 585, Kanagawa 1986, p. 355). The angle theta, θ, has been variously defined as the angular difference in trend (azimuth) between the trace of a bulk mean cleavage and the trace of the axial surface or trend of the fold axis (Stringer & Treagus 1980, Craig 1985, 1987, pp. 174–176, Mackie 1987, fig. 4.1, Wilkinson 1988, fig. 4.13 and Fig. 5 of this paper, angles b and c, respectively). These measures should not be used because of possible ambiguities in the apparent sense of axial-transection brought about by the complexities in fold axial surface shape, difficulty in definition of the axial surface trace in variably (or steeply) plunging asymmetric folds and topographic effects. For instance, Fig. 6 shows stereographic representation of cleavage and an axial plane of constant attitude. Fold axes plunge variously within the axial plane (i–iv) so that Δ varies (g, f, zero and h, respectively). The sign of Δ is negative (clockwise axial-transection) for i and ii but positive (anticlockwise) for iv. However, if θ is used as a guide to the sense of axial-

transection (a–e) then all folds (i–iv) would be classed as clockwise axially-transected.

Powell (1974) showed aggregated cleavage and axial plane poles and traces which were not coincident within the fold profile plane (figs. 6d, 8d and 12 in Powell 1974). This suggests a bulk profile transection of folds by the cleavage (d-type). He also produced an equal-area projection of a fold whose π-axis did not lie within the bulk cleavage plane, suggesting Δ/t transection (his fig. 17d). Stringer & Treagus (1980), when describing cleavage-transected folds from the Southern Uplands, used the "dihedral angle between axial surface (*sic*) and mean plane to S_1 cleavage fans", found stereographically. However, their "axial surface" was measured using the inflection point method and is therefore a limb-bisector surface. Possible variations in β (Hudleston 1973) are ignored. King (1987 and personal communication) also measured this dihedral angle but, instead, used the fold axial plane (Fig. 5, angle m). The measure is independent of the pitch of the fold axis within the axial plane and, thus, will only be equivalent to Borradaile's Δ (and t) if d is zero. Since this angle cannot be measured directly but can be calculated, given Borradaile's Δ and d, it is unnecessary.

Descriptions of cleavage-transected folds are given by Ramsay (1963) and Moench (1970) who stated that cleavage crosses or cuts the fold axial surfaces and both limbs. This indicates non-zero Δ/t fold transaction, Duncan (1985) in his re-evaluation of Powell's (1974) area described combined Δ/d transective geometry without quantification. Cameron (1981) described cleavage–fold

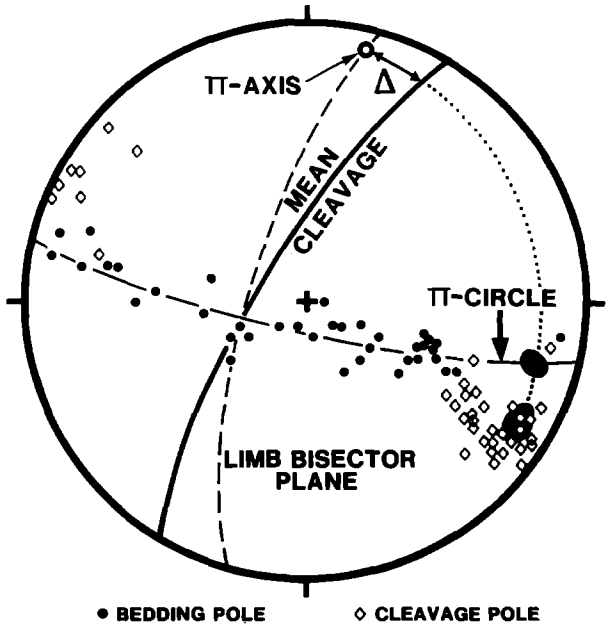

Fig. 7. Equal-area projection showing determination of Δ and d^* from aggregated measurements of folds at Pont Rhyd-y-Groes, Dyfed, Wales. Bedding poles define a non-random girdle at the 99% level of confidence (n = 38, k = 0.1768, S_1/S_3 = 92.46 and eigenvector 3 = 9/013). Cleavage poles define a non-random cluster at the 99% level of confidence (n = 41, k = 1.8515, S_1/S_3 = 61.55 and eigenvector 1 = 13/121). d^* is the inter-trace angle between LBP and the mean cleavage plane in the π-circle. In this case the traces are coincident so that apparent profile-transection is zero or $d^* = 0$ and therefore $\Delta = t^*$ (type B*, Fig. 12b). Bulk Δ is measured in the plane containing the π-axis and the mean cleavage pole and is −15° in this example (see Fig. 13). Filled elliptical areas are cones of confidence for mean cleavage and the normal to the π-axis cone within the plane containing both mean cleavage and π-axis (confidence level is 95%).

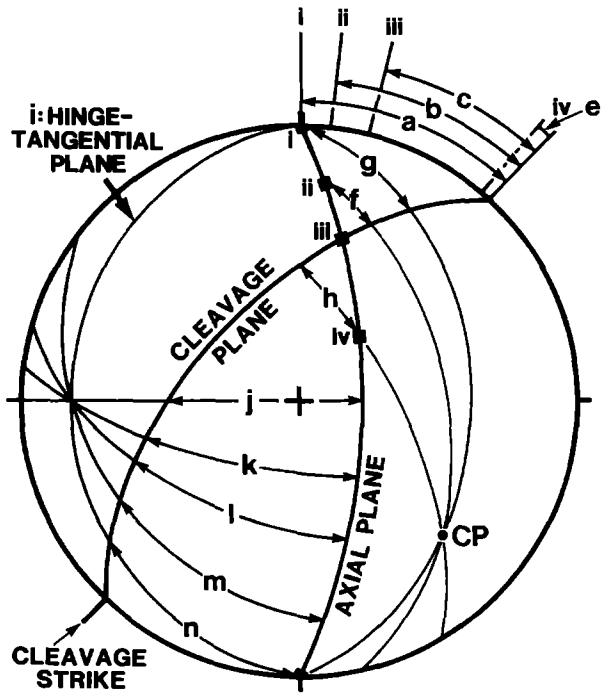

Fig. 6. Lower-hemisphere equal-area projection of cleavage and axial plane of constant attitude with variable fold axis plunge (i–iv), a–e represent resulting variable θ values; g–h, variable Δ; j–m, d values; and n, the t value for fold i.

geometries consistent with pure Δ/t-type and combined Δ/d-type transection but also did not quantify the relationships. Murphy (1985) redefined Δ as "the dihedral angle between the trend of the cleavage–bedding intersection and the fold axis measured in the plane of the deformed bedding". Cleavage–bedding intersections will define a complex non-parallel array in axially transected folds (Powell 1974). Presumably, "bedding" here refers to the enveloping or median surface and "cleavage–bedding intersection" to the intersection of the mean cleavage with this plane. If this is the case then the measure is equivalent to Treagus & Treagus's Δ (see below and Fig. 5, angle f) but not to Borradaile's Δ. The 'T' measure of Soper (1986), Soper *et al.* (1987) and Woodcock *et al.* (1988) is equivalent to Borradaile's Δ, differing only in that it is measured using a bulk mean cleavage pole from an area rather than individual cleavage planes (Fig. 7). Bell (1978), Gray (1981), Dias (1986), Anderson (1987), King (1987), Blewett & Pickering (1988), Lafrance (1989) and Woodcock (1990) apparently used Borradaile's Δ as defined. Although Anderson (1987), Williams (1985) and Williams & Urai (1989) described Δ/d-type transective relationships, only Gray (1981) attempted to measure d. Other authors have reported "transected folds" without quantification (Storey & Nell, 1988).

Soper (1986), whilst describing anastomosing or

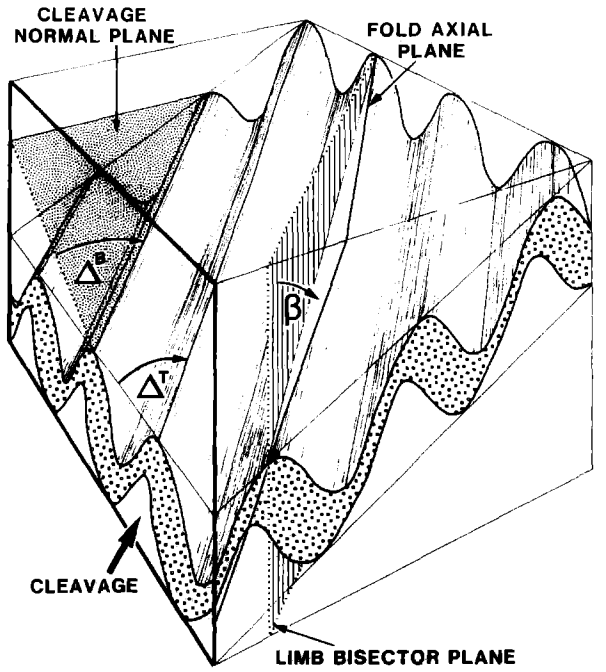

Fig. 8. Upward-facing asymmetric folds enclosed by their enveloping surfaces within which fold axes pitch moderately. Limb-bisector and fold axial planes are non-coincident. An anticlockwise axially-transective cleavage is shown. Borradaile's measure, Δ^B is measured in the plane containing the cleavage normal and fold axes, whereas Treagus & Treagus's measure, Δ^T, is measured in the enveloping surface. They are different angles.

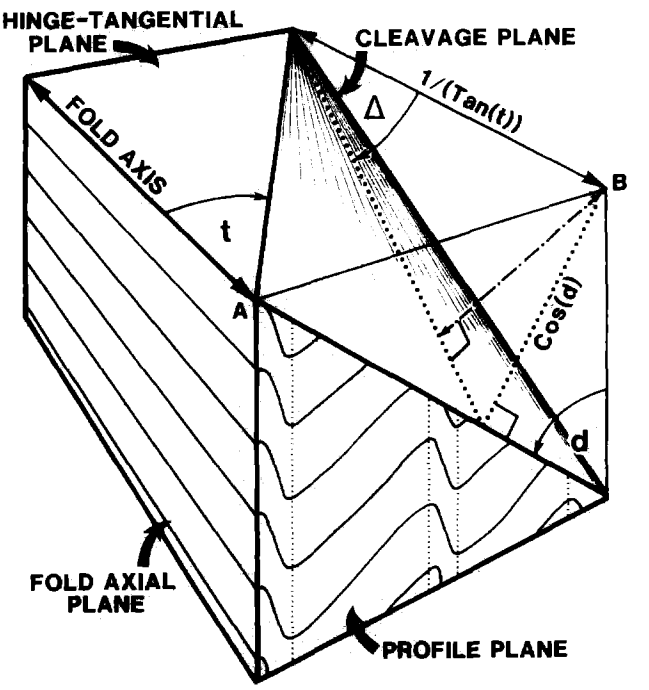

Tan(Δ) = Tan(t).Cos(d)

A-B=UNITY

Fig. 9. Trigonometric calculation of t where Δ and d have been measured. If the fold axial plane cannot be determined, then a limb-bisector plane is used and t and d become t^* and d^*. Measures t and d are equal to t^* and d^* only if the fold axial plane and limb-bisector planes are coincident. The method of calculation is similar in both cases and the value of Δ is unaffected by the plane used.

'rough' cleavages in arenites, used an angle Δ (not equivalent to Borradaile's Δ) to describe the amount of cleavage dispersion in various planes (profile, bedding, hinge-tangential plane, etc.).

Treagus (1982) used an angle β between the cleavage trace and bedding normal within the profile plane (Fig. 5, angle k) for two-dimensional classification of foliated folds. To achieve this β was graphed against a normalized bedding dip angle. The quantity d can be simply derived from such plots but the plots ignore axial-transection (Δ-type).

Theoretical modelling

Coaxial strain models proposed by Borradaile (1978) and Treagus & Treagus (1981) were three-dimensional. Borradaile (1978) defined the theoretical angle delta δ as "the angle between the principal extension in the surface" undergoing folding, "and its projection in the XY plane". Treagus & Treagus (1981, p. 4) redefined Borradaile's Δ as "the angle between the bulk XY plane and the fold axis measured in the plane of the deformed layering ... the enveloping surface or median surface after folding" (Fig. 5, angle f). This is not equivalent to Borradaile's Δ or δ, which are both angular projections of lines onto planes. It will be equivalent to t (and t^*) only if folds are symmetrical. Otherwise it is a separate measure (Fig. 8). (They suggested that the plane in which Borradaile measured Δ is not specified. In fact Borradaile clearly stated that it is measured in the plane

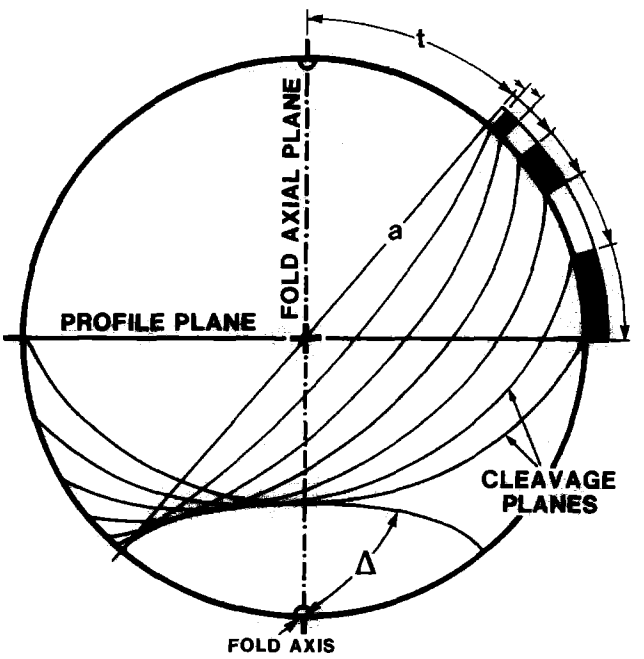

Δ : CONSTANT, d : AT 15° INTERVALS, t : VARIABLE.

Fig. 10. Lower-hemisphere equal-area projection for theoretical fold with cleavage planes at constant Δ angle to the fold axis. Increments of d at 15° and the resulting magnitude of t are shown. Where $d = 0$ (cleavage plane a) then $t = \Delta$. As d increases from zero, the increase in t relative to Δ grows (see Fig. 12a). If the fold axial plane is replaced by a limb bisector plane, t and d become t^* and d^*.

containing the fold axis and its projection onto the cleavage plane.) Non-coaxial strain models to account for fold axial-transection by cleavage (fig. 2 in Soper, 1986, fig. 4 in Soper *et al.* 1987, fig. 8 in Sanderson *et al.* 1980) are two-dimensional and assume bulk d to be zero so that $\Delta = t$.

Discussion of nomenclature

As is apparent from the above examination, nomenclature describing cleavage-transected fold geometry has been confused. The main problem has been a tendency for new workers to redefine old measures to suit particular circumstances of outcrop, data availability or theoretical modelling in each case. Methods of measurement have not been clearly and unambiguously described, precluding comparison of measurements among areas. Newly defined measures were given symbols previously used for different measures, adding to the confusion. Measures used in theoretical studies have not always been practicable for field data processing. This has prevented direct comparisons of predicted and real cleavage-transected fold geometries.

Some confusion has been caused by a slackness in usage of purely vectorial vs physical/descriptive terms to describe folds. "Fold hinge" describes a physical geometric feature on the folded surface: the locus of points joining areas of maximum surface curvature. "Fold axis", on the other hand, is a direction (vector) (defined by π- or beta-diagrams) which may have no physical expression on the fold. Therefore, observed hinge-transection of high-order folds does not necessarily imply fold axis- (or hinge-) transection of lower-order folds in the same area (for example, Lafrance 1989).

A problem arises with non-cylindrical, for example en échelon, folds because the individual folded surfaces may not always contain the π-axis. The derived mean profile plane (best-fit π-circle) may therefore be oblique to the profile planes of individual folds. This problem may be shown up by separating individual fold, or limb, bedding-pole distributions on the stereonet. This should reveal any possible pattern to the non-fit of bedding-poles to the best-fit great circle. Such factors may give rise to very small errors in profile-transection measures and potentially larger ones in Δ. These errors are perhaps less than those caused by the often invalid assumption that axial surfaces are planar. Curved axial surfaces give rise to curved axial surface traces which are difficult to define precisely without a large amount of data.

It should be noted that measurement of Δ alone does not define the value of either d^* or t^*. If folds approximate to monoclinic symmetry then Δ and d^* must be quantified; t^* can then be calculated if necessary (Fig. 9).

Isogonic lines of t^* (or t if the fold axial plane is known) are shown on the Gray plot of Δ vs d^* (or d, Fig. 12 and see below). The magnitude of Δ is seen to depend on both d^* and t^*. Hence, where profile transection is high then Δ gives a large underestimation of t^* (Fig. 10).

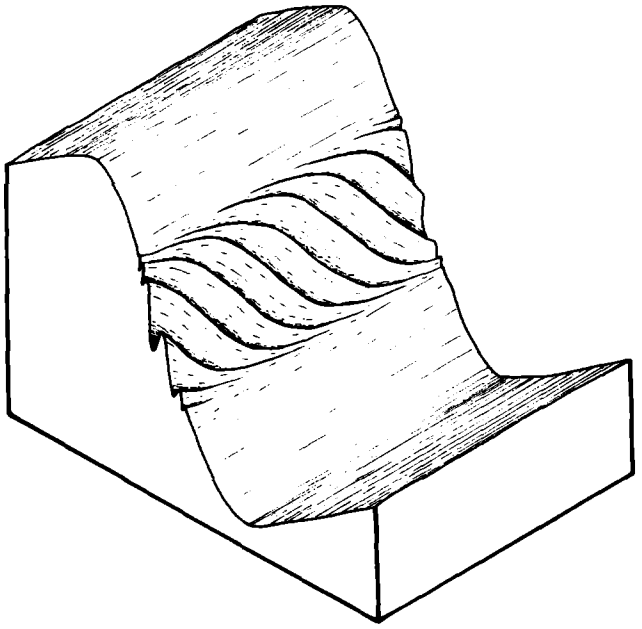

Fig. 11. A possible fold geometry in which relatively short wavelength folds have developed preferentially on the most steeply dipping part of a larger wavelength fold limb. The bedding on the limbs of the minor folds will strike clockwise of the general bedding strike. Cleavage may be axial planar to the minor folds and yet clockwise axially-transect the larger amplitude folds. The apparent magnitude of this transection will, to some degree, be determined by the sampling of the structures.

SCALE OF OBSERVATION AND SAMPLING

Scale of observation

It is clearly of little practical use to compare microscopic cleavage-parallel mica orientation with oroclinal bend axes or indeed to compare regionally-averaged cleavage orientations with microscopic mica kink folds. The features being compared must be clearly related and of comparable scale for results to be meaningful. The structures being compared must be stated and fully described. The relationship between folds and cleavage is not always clear and therefore cleavage measured at one scale must be compared with folds of various orders. Generally folds of different wavelengths do not have coincident axial features.

Should relationships between 'individual' cleavage planes and fold axes be examined? Or, are bulk, averaged cleavages to be used? The definition of 'a cleavage plane' is itself a scale-related concept. What is measured at outcrop as a cleavage plane may in fact be a composite of two or more microscopic fabrics along which a joint has formed. A microscopic examination of rough cleavage in arenites may reveal an irregular anastomosing network of cleavage seams (Soper 1986) whose mean mesoscopic attitude reveals little about the orientation of microfabric elements. Therefore, there are implicit assumptions in measuring cleavage at different scales. For instance, at outcrop it is assumed that clinometer measurements average out grain-scale fabric variations. This is only likely to hold true in fine-grained slates. Bulk, vector-mean cleavage poles using eigenvector

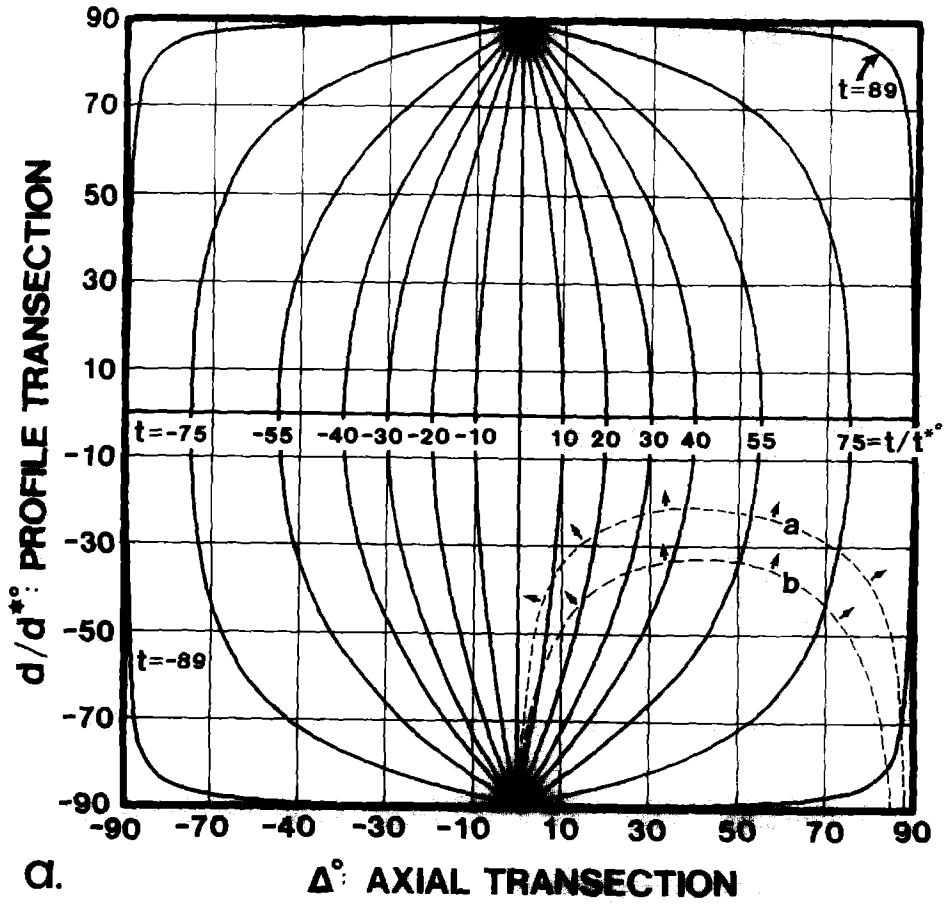
90
70
50
30
10
-10
-30
-50
-70
-90
t=89
t=-75
-55
-40 -30 -20 -10
10 20 30 40
55
75=t/t*°
a
b
t=-89
d/d*°: PROFILE TRANSECTION
-90 -70 -40 -30 -10 10 30 50 70 90
Δ°: AXIAL TRANSECTION
a.

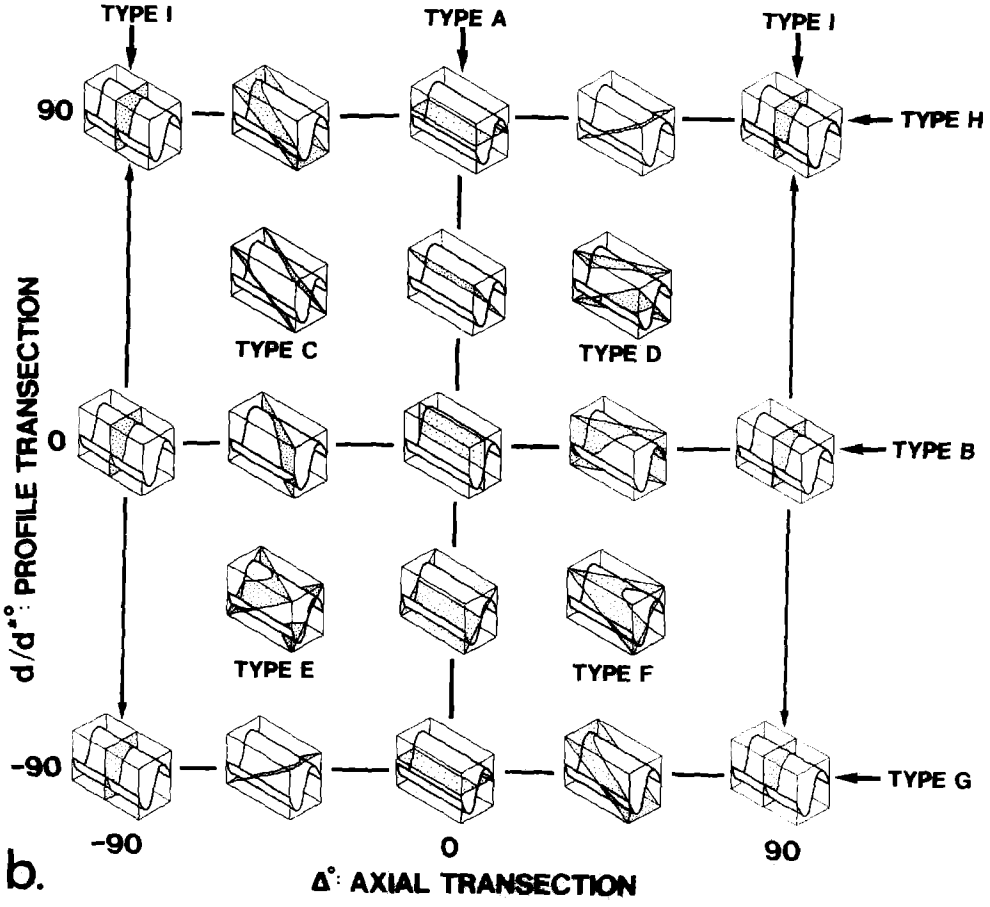
TYPE I
TYPE A
TYPE I
90
TYPE H
TYPE C
TYPE D
0
TYPE B
TYPE E
TYPE F
-90
TYPE G
d/d*°: PROFILE TRANSECTION
-90
0
90
Δ°: AXIAL TRANSECTION
b.

Fig. 12

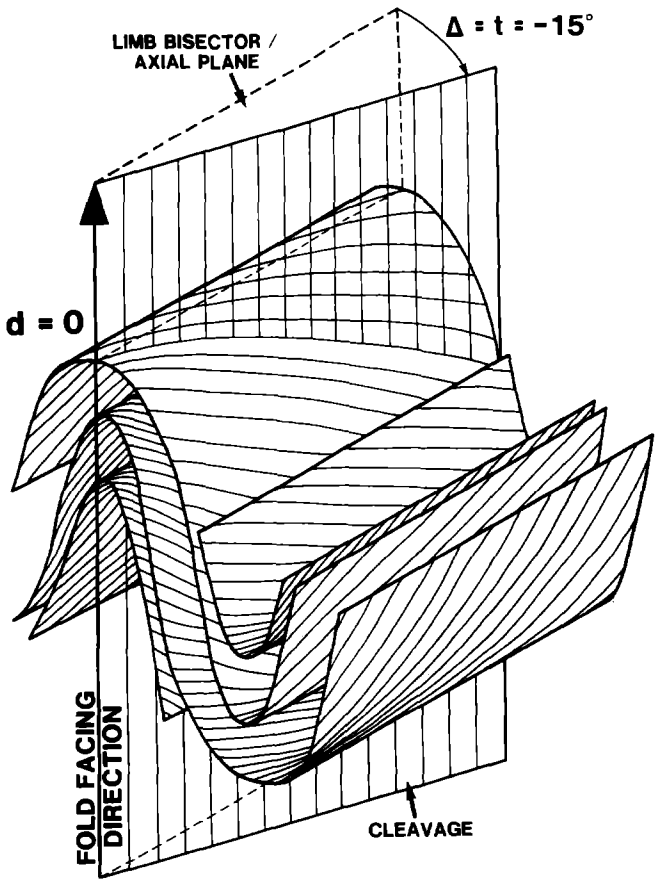

Fig. 13. Folded surfaces transected by a vertical cleavage which is parallel to the intersection of profile and axial planes. This is a case of pure Δ/t-type transection (type B of Fig. 12b) where $\Delta = t = -15°$ (see Fig. 7).

calculations are assumed to 'average out' refraction effects. This will only be the case if sampling is even and unbiased and refraction symmetric about the fold axial plane/limb-bisector plane. It is informative to examine the sub-fold scale components of bulk axial transection, that is measured cleavage plane data.

Sampling

Non-targeted sampling of a three-dimensional fold exposed in an effectively two-dimensional restricted outcrop will often be biased in some respect (Whitten 1966). The hinges of angular, upright folds are relatively unlikely to be sampled because, volumetrically, the structures consist largely of fold limbs. Gently dipping surfaces occurring within the hinge-zones are also difficult to measure accurately (Woodcock 1976). Hinge-zones may be composite structures comprising en échelon parasitic folds, whereas the main fold limbs are relatively unaffected by these oblique structures (Moseley 1962). Therefore if sampling density is constant then limb-biased π-circle patterns may result. Generally, limited outcrop will determine sampling locations. The outcrop distribution is usually controlled by a complex interplay of geological and geomorphological factors. This may introduce an appreciable bias into structural data sets. Other potential structural contributions toward sampling bias include relatively high-order (often partly conical or en échelon) folds, with relatively short wavelength and limited spatial extent, parasitic on lower-order (sub-cylindrical) folds (Fig. 11) (Campbell 1958), asymmetric folds, lateral-linking folds and bifurcating fold hinges (Dubey & Cobbold 1977). Whether such features produce detectable anomalies on π-circle plots will depend on the spacing of sampling stations, and the size and frequency of the anomalous folds (Sanderson 1973). There is usually an unstated sampling bias toward those lithologies whose character facilitates measurement of particular structures. For instance, in turbiditic sand–silt–mudstone sequences cleavage is often best developed and therefore most easily measured in mudstones. In long-exposed hill-side exposures, rough cleavage in immature sandstones may be well exhibited, though apparently absent in fresh outcrops (Smith 1987). Conversely, quartzose siltstone may appear uncleaved except in thin section. Measurement of bedding is also prone to unwitting bias. Competent beds, resistant to weathering, provide good surfaces for clinometer readings. In wholly right-way up sequences there is an obvious bias toward the tops of beds. Some turbiditic sandstones have cross-bedded tops which may introduce a directional bias to bedding measurements. Gross features of the sediment body geometry of sandstones such as scours and lateral accretion surfaces may similarly introduce bias. Differential sampling of these structures is generally inevitable and therefore their presence should be recorded and borne in mind during interpretation. However, large sample size, gridded sampling or selection of particular well-exposed lithologies or horizons for detailed analysis all act against, without eliminating, biased sampling.

Fig. 12. (a) Gray's plot of axial-transection vs profile transection. Isogonic lines for hinge-tangential plane (or limb-bisector/profile-normal plane) transection angles are calculated from the relationships shown in Fig. 9. The plot shows that t/t^* cannot be zero if Δ is non-zero. The broken lines 'a' and 'b' delimit areas outside of which Δ diverges from equality to t/t^* by less than 2° and 5°, respectively, for that quarter of the diagram. (b) Geometric classification of specific or bulk cleavage measurements on upward-facing folds using the Gray plot. The folded surfaces shown are examples only. Folds with other interlimb angles and symmetries may equally-well be classified using the diagram. Types C–F represent the general case where components of both d-type and Δ-type transection occur. If required, these fields may be subdivided into areas lying above or below the $t = d$ or $t^* = d^*$ lines (Fig. 14a), subdividing transecting cleavages into those that are dominantly profile-transective from those that are dominantly axially-transective, respectively. All non-type A relationships are axially-transective. Note that cleavage–bedding intersections plunge in opposing directions for type B transected folds and where d is low for types C–F. With increasing d-transection they may plunge in the same general direction on both limbs of the fold (depending on the interlimb angle) but are never parallel to the fold axis. The plot includes downward-facing cleavages which will occupy an increasingly large area as interlimb angle decreases.

TREATMENT OF CLEAVAGE-TRANSECTED FOLD DATA IN STEREOGRAPHIC PROJECTION

Bulk treatment of data

Cleavage and bedding measurements are collected from the area of interest. Sub-areas showing internally consistent fold and cleavage orientations may be selected. This will be the case, for instance, in areas whose plotted bedding-poles define girdles at the 99% level of confidence. Cleavage- and bedding-pole data are separately analysed by the eigenvector method (Woodcock 1977). The eigenvalue ratio $S_1 : S_3$ is used to ensure that bedding-poles define a statistically non-random girdle and cleavage a non-random cluster at the 99% level of confidence (Woodcock & Naylor 1983). This level of confidence should filter out areas affected by non-cylindrical folding (assuming sampling to be unbiased). Bulk equivalents of Δ (T of Soper *et al.* 1987) and d^* (and therefore t^*) can then be calculated using the π-axis (eigenvector 3 of bedding poles), and vector-mean cleavage pole (eigenvector 1 of cleavage and Fig. 7).

Ideally, two-sample statistical tests should be made of the hypothesis that the mean cleavage pole and π-axis normal in their mutual plane do not coincide. If they coincide then t/t^* and Δ are zero. The Bingham distribution (Bingham 1974) could be used as a model in such tests, with the drawback that it assumes orthorhombic symmetry. In the absence of useful tests, cones of confidence are calculated for the mean cleavage (assuming a Fisher distribution) and π-axis (assuming a Bingham distribution, Cheeney 1983 and Fig. 7). An error cone (95% confidence level) normal to the π-axis cone is constructed in the plane containing the π-axis and mean cleavage pole. If the two cones overlap, then the fold is said not to be (bulk) axially-transected. Otherwise a range of bulk Δ values can be given and the folds are said to be bulk axially-transected by the cleavage.

High resolution geometry of cleavage-transected folds

The measures Δ and d/d^* are found stereographically (Fig. 4) or by trigonometric calculations (Fig. 9) in the way described above. Cleaved folds formed in multi-layer sequences usually show refraction of cleavage surfaces across layer (viscosity) boundaries. Lower-order fanning of the cleavage around the fold is also common. These are both profile-transective relationships. Bulk structural analysis of such features (Fig. 7) relies upon the assumption that fanning and refraction are symmetrical about the fold axial plane/limb-bisector plane and that, if sampling is thorough, then such effects will be self-cancelling, i.e. the mean cleavage pole will equally take account of fanning and refraction on both limbs of folds. Cleavage refraction is currently viewed as being due to either XY plane-tracking of cleavage while differential strains are imposed on folding layers of varying viscosity (Ramsay & Huber 1983, p. 184) or to variable deformation of an orthogonal pre-buckling fabric imposed during layer-parallel shortening (e.g. Henderson *et al.* 1986). Whatever processes dominate, asymmetrical folds are unlikely to have been subjected to equal components of these processes on long and short fold limbs. Therefore, aggregating the cleavage data may be very misleading for such folds. Most folds in orogenic belts show asymmetry on some scale. The analysis of the degree of asymmetry of cleavage refraction on different limbs of the same fold should provide information useful in interpreting the relative timing of folding and cleavage formation or, at the least, the relative contributions of buckling and cleavage formation to the finite strain state.

Analysis of the relative arrangement of individual measured cleavage planes within folds involves graphical comparison of d (or in practice d^*) and Δ measures (Gray 1981 and Fig. 12a). Specific cleavage 'plane' orientation with respect to fold axial features should provide useful information on the contributary factors to bulk fold axial transection in an area—for instance, whether the degree or sense of axial transection remains constant on different fold limbs or parts of limbs.

Fabric geometric analysis could follow this general scheme and relate mica fabric and pressure solution seam orientation to associated (oriented) micro- and meso-folds. The study of anastomosing or 'rough' cleavages is facilitated by such methods.

'GRAY' GRAPH OF Δ VS d

Gray (1981) suggested that Borradaile's Δ and d measures could be graphed for aggregated data from folds. Its use may be extended so that specific cleavage measurements can be compared with associated fold features in areas where full profile exposure does not occur. Because of the problem of fold axial plane location already described, d^* is plotted against Δ. This reveals useful information about the geometric elements contributing to the bulk transection seen in previous studies (Soper *et al.* 1987, Woodcock *et al.* 1988). Hitherto, such comparisons have largely been restricted to qualitative estimates based on bedding trace and fold axial surface trace obliquity to cleavage trace (p. 551 and fig. 1 in Price 1962) or stereographic analysis (Stringer & Treagus 1980, p. 326).

Figure 12(b) is a Gray plot of Δ against d/d^* showing the main geometric types of fold-transecting cleavages. Two main end-member geometries for transected folds were defined by Borradaile (1978): (i) pure profile-transected folds in which the cleavage contains the fold axis direction but transects the fold axial plane trace in fold profile view ($d/d^* \neq 0 = \Delta = t/t^*$, type A); (ii) pure axially-transected folds in which the cleavage is parallel to the axial plane trace in profile but cuts across the fold axis ($d/d^* = 0 \neq \Delta = t/t^*$, type B). In this case the

cleavage contains the fold axis normal which lies in the fold axial plane or limb-bisector plane, i.e. it is parallel to their traces in the profile plane (Fig. 13). The general case (iii) will be that in which the bulk cleavage contains neither the fold axis nor the fold axial plane/limb-bisector plane trace in the profile plane (types C–H). This classification applies to folds with orthorhombic symmetry where $d = d^*$ or those of lower symmetry classes where d^* is used. Since the various geometric types on the $\Delta - d$ plot may not coincide with those on the $\Delta - d^*$ graph, they are renamed type A*, B*, etc. This classification may be applied to the treatment of 'individual' cleavage planes or bulk data from various sub-areas.

Method of plotting

The values of d/d^* and Δ for measured cleavage planes are found stereographically for a single fold or closely associated folds. To aid comparison there is a need for consistency of d/d^* sign convention throughout the area. Therefore, folds are viewed along their axes in a consistent direction when deciding the sense of 'rotation' of cleavage traces relative to fold axial plane trace/limb-bisector plane trace (Fig. 4). Locality codes may then be plotted at the relevant point on the graph. Sampling of individual folded layers (inner and outer arcs) from hinge to inflection points is desirable although rarely possible. In this case readings at intervals can be plotted and linked on this construction to show the sequence of transective geometry changes across the fold.

It is also desirable to differentiate layers of different viscosity and convergent and divergent cleavage fans (Fig. 15b). High-resolution $\Delta - d/d^*$ plots allow determination of the various dispersion angles (Δ of Soper 1986) of anastomosing or 'rough' cleavage if enough readings have been collected (in the field or from microscopic examination of orientated sections—see Fig. 15a). Such studies help to detail lithology-dependent variations in the range of axial- and profile-transection. This aids interpretation of possible mechanisms of formation.

Bedding dips and dip directions from cleavage sample localities may be plotted on the graph at the relevant points (Fig. 15a). This allows investigation of any proportionality between bedding dip and the transection measures. It is perhaps more useful to plot bedding dips after rotation of the computed fold axis to horizontal (and—if possible—fold axial plane/limb-bisector plane to vertical). The bedding planes perpendicular to the limb-bisector plane trace in the profile plane can be used as a datum (apparent hinge zone). The apparent hinge zone may be slightly offset from the true hinge zone, usually towards the short/thinned limb. The symmetry of cleavage fanning and refraction relative to this zone can then be seen directly (Figs. 14 and 15). The apparent hinge readings may not plot on the $d^* = 0$ axis or lie symmetrically about it (Fig. 14). Variations in the degree of such offset should be interpreted with caution because they may result from: variations in β, sign changes in t^* and Δ resulting from use of the limb-bisector plane as datum, sampling bias, variable degree of hinge migration or departures from the assumed fold symmetry. For instance, the hinge-tangential plane may not be parallel to the tangential plane perpendicular to the limb-bisector plane (see asymmetric, imperfect folds of Twiss 1988). Apparent hinge-zone offset in asymmetric folds usually represents a non-zero situation of β, where $d^* \neq d$. If the vergence and sense of relative limb attenuation is consistent in an area then the direction of apparent hinge-zone offset ($\pm d^*$) may also remain constant. Many folds should be measured to detect any consistent sense of offset rather than that which might arise—for instance—from local axial surface undulation, oblique-linking folds or bifurcating hinges of non-cylindrical folds. Some offset may result from hinge rolling/migration. The direction of hinge migration would be expected to be toward the limb in the offset direction in antiformal-convergent or synformal-divergent cleavage fans and away from that limb in synformal-convergent or antiformal-divergent fans (sense of Ramsay 1967, p. 405). However, it is questionable whether such D–d^* plots have the resolution to detect and distinguish apparent hinge-zone offsets due to hinge migration from those resulting from β variations.

It should be noted that the problems associated with non-coplanarity of axial plane and limb-bisector plane will, normally, only result in point positions shifting parallel to the d/d^* axis. This is because the absolute magnitude of Δ is independent of how profile-transection is measured. However, more complex pattern changes occur if cleavages are highly profile-transective. This means that unless facing information is available, the plot cannot be used to analyse cleavages at a small angle to bedding, which cleavages, because of hinge migration, are now highly profile-transective.

Cleavage–bedding intersection plunges can be plotted at the corresponding Δ/d^* co-ordinates to allow comparison of plunge of the intersection with the relative magnitudes of Δ and d^* (Fig. 15b).

Cleavage point distributions may be classified and described using the following features: (i) number of fields which the point spread occupies; (ii) shape of the spread (e.g. linearity, shape of curved spreads and comparison with $t^* = d^*$ and isogonic t^* lines, see Figs. 14a & c); (iii) degree of symmetry of the spread with respect to d^* or Δ axes (Fig. 14b); (iv) ratio of the Δ range to the d^* range (Fig. 15a); (v) ratios of $+\Delta:-\Delta$ and $+d^*:-d^*$ (Fig. 15a); (vi) position of the apparent hinge-zone cleavage readings with respect to the d^* and Δ axes (Fig. 14); (vii) sign of slope of the point spread; (viii) relative shapes of convergent and divergent cleavage fans (Fig. 15b); or (ix) the distribution of upward- and downward-facing cleavages (Shackleton 1958) on the plot. Given the probable variation of β in natural folds, interpretation of subtle variations of point plot shape are probably not justified. The general form of the distribution should, however, be quite close to that of the true $\Delta - d$ plot.

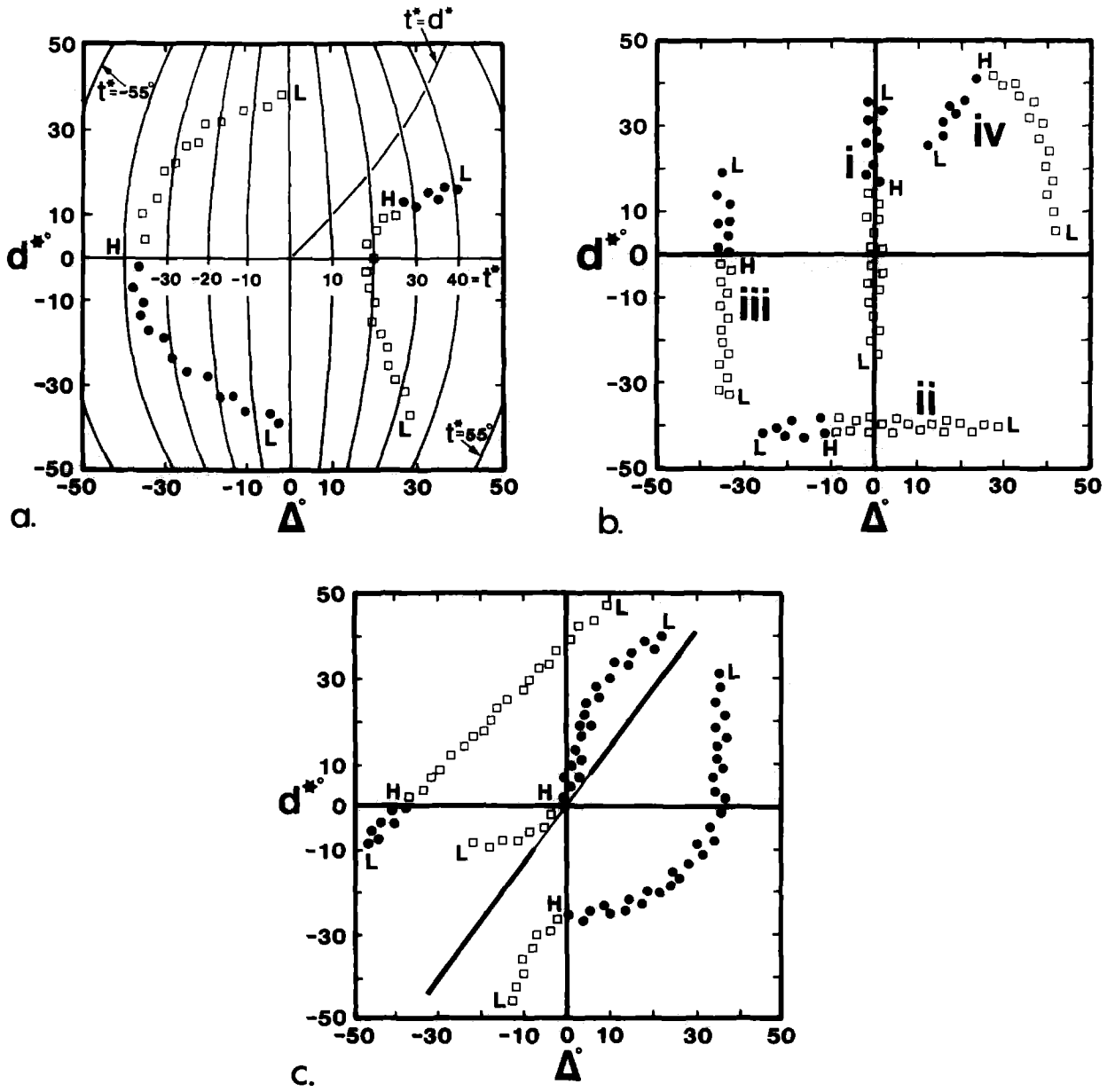

Fig. 14. Limb-separated cleavage data for imaginary folds. 'H' represents the apparent hinge zones and 'L', inflection zones. (a) Gray plot with isogonic lines for t^*. Plots of measured cleavages should not include those whose poles fall between limb-bisector plane and fold axial plane great circles (Fig. 5, planes r and q). In other words, cleavages with $d > (90 - \beta)$ (Hudleston 1973) should be excluded. If β is not known then highly profile-transective (e.g. $d > 55°$) should be excluded or interpreted in the light of an assumption of low β. This is necessary because such cleavage planes will have Δ and d signs that will change, resulting in gross distortions of the point pattern on the plot. (b) & (c) Gray plots showing point distribution features of use in classifying real fold data.

Within a region, fold axes, fold axial planes/limb-bisector planes and cleavage pertaining to folds of various scales can be used as the basis for Gray plots to suggest which folds were most active during cleavage formation. Those folds whose convergent-fanning cleavage plots show point distributions with the greatest d^* range are likely to have been the most actively growing during (and after) cleavage formation (Fig. 14bi). In multilayer sequences with viscosity contrasts, d (and d^*)-type transection should greatly exceed Δ/t-type transection resulting in a point plot which is somewhat elongate parallel to the d^* axis (Figs. 14bi & iii). However this is not necessarily the case in folded sequences of 'homogeneous' viscosity (e.g. thick mudstones). The most active fold order is likely to vary with depth in the deforming pile, geometry and viscosity of multilayers, proximity to major shear zones, position along progressive deformation path, etc. Therefore, the number of fields occupied by the point spread only provides a very approximate indication of the relative timing of cleavage formation with respect to folding if lithology and other factors are taken into account. If downward-facing cleavage occurs then true overprinting must be suspected, although it might occur in cleavage-transected folds in which significant hinge migration has taken place or where parasitic downward-facing folds occur on the overturned limbs of otherwise upward-facing, lower-order folds.

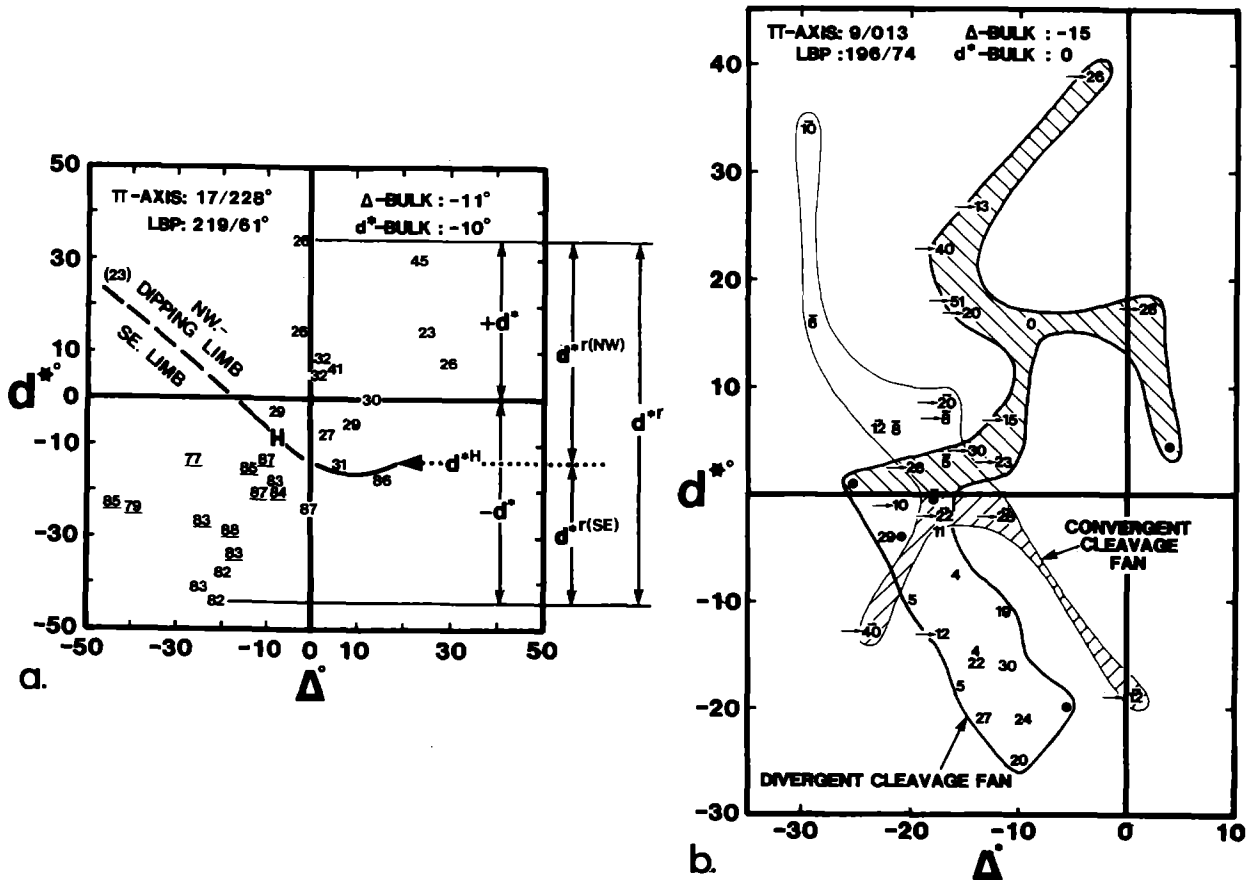

Fig. 15. Folds from the low-grade Late Caledonian–Acadian fold belt of Wales. The sign of d^* is found whilst viewing along fold axes toward the NE (Figs. 4 and 5). (a) Gray plot for the SE-vergent Berwyn Anticline at Llyn Efyrnwy, Powys, Wales (SJ020197–024192). This is an angular, cleaved fold in the Caradoc siltstones and tuffs of the Pen plaenau Siltstone Formation, Swch Gorge Tuff and Allt-tair-ffynnon Formation. The fold is close with a steeply inclined axial plane, hinge gently plunging to the SW, and a wavelength of 11 km. Bedding dips (in degrees) are plotted at the d^*/Δ position for the corresponding cleavage plane measurement. Underlined numbers indicate overturned bedding. 'LBP' indicates limb bisector plane. The range and symmetry of profile-transection may be specified using the parameters d^{*r}, $+d^*$, $-d^*$, d^{*H}, $d^{*r(NW)}$, $d^{*r(SE)}$ as shown, and the ratios $+d^*:-d^*$ and $d^{*r(NW)}:d^{*r(SE)}$. A similar scheme can be adopted for describing axial-transection: Δ^r, $-\Delta$, $+\Delta$, etc., or t^{*r}, $-t^*$, $+t^*$, etc. (b) Gray plot for folds at Pont Rhyd-y-Groes, Dyfed, Wales (SN 748731–750733). The data are aggregated for a few close, approximately 10 m, wavelength, SE-vergent, steeply inclined and sub-horizontal folds. Rocks affected are cm-bedded siltstone–mudstone turbidites of the Telychian (Late Llandovery), Devils Bridge Formation. Cleavage–bedding intersections readings are shown at the Δ/d^* positions for corresponding measured cleavage planes. Convergent-fanning cleavage points are overlined, whilst divergent-fanning cleavages are not. Hatched areas represent readings from SE-dipping limbs; NE–SW hatch for convergent fans and NW–SE for divergent fans. Apparent hinge-zones lie on or near the $d^* = 0$ axis. Cleavage–bedding intersections plunging more steeply than the π-axis, to the NE, are arrowed. Cleavage readings where no cleavage–bedding intersections were measured are shown as circles. 'LBP' is the limb bisector plane (found using the inflection point method).

CONCLUSIONS

(1) Confusion in past analyses of cleavage-transected folds has resulted from repeated redefinition of measures. The nomenclature is clarified here and extended to allow measurement of geologically realistic asymmetric folds.

(2) Sampling of asymmetric folds in areas of restricted outcrop may well be biased. Such bias should be considered when interpreting structural survey data.

(3) 'Gray' plots of axial-transection vs profile-fold-transection by cleavage provide a powerful means of investigating the detailed consitutive geometry of cleavage-transected folds. Their use can be extended to include specific cleavage data.

(4) The Gray plot should, in future, aid interpretation of the progressive development of cleavage-transected folds.

Acknowledgements—This work was carried out whilst in receipt of Natural Environment Research Council Studentship GT4/86/GS/114 under the supervision of Nigel Woodcock (University of Cambridge), whose helpful criticism is gratefully acknowledged. Discussions with Steven King (Queen's University of Belfast) on CTF measures are much appreciated.

REFERENCES

Anderson, T. B. 1987. The onset and timing of Caledonian sinistral shear in County Down. *J. geol. Soc. Lond.* **144**, 817–825.

Anderson, T. B. & Cameron, T. D. J. 1979. A structural profile of Caledonian deformation in County Down. In: *The Caledonides of the British Isles—Reviewed* (edited by Harris, A. L., Holland, C. H. & Leake, B. E.). *Spec. Publs geol. Soc. Lond.* **8**, 263–267.

Bell, T. H. 1978. The development of slaty cleavage across the Nackara Arc of the Adelaide Geosyncline. *Tectonophysics* **51**, 171–201.

Bingham, C. 1974. An antipodally symmetric distribution on the sphere. *Ann. Stat.* **2**, 1201–1225.

Blewett, R. S. & Pickering, K. T. 1988. Sinistral shear during Acadian deformation in north-central Newfoundland, based on transecting cleavage. *J. Struct. Geol.* **10**, 125–127.

Borradaile, G. J. 1978. Transected folds: a study illustrated with examples from Canada and Scotland. *Bull. geol. Soc. Am.* **89**, 481–493.

Campbell, J. D. 1958. En échelon folding. *Econ. Geol.* **53**, 448–472.

Cameron, T. D. J. 1981. The history of Caledonian deformation in East Lecale, County Down. *J. Earth Sci., R. Dublin Soc.* **4**, 53–74.

Cheeney, R. F. 1983. *Statistical Methods in Geology*. George Allen & Unwin, London.

Considne, D. M. (editor). 1976. *Van Nostrand's Scientific Encyclopaedia* (5th edn). Van Nostrand Reinhold, Scarborough, California.

Craig, J. 1985. Tectonic evolution of the area between Borth and Cardigan, West Wales. Unpublished Ph.D. thesis, University College of Wales, Aberystwyth.

Craig, J. 1987. The structure of the Llangranog Lineament, West Wales: a Caledonian transpression zone. *Geol. J.* **22**, 167—181.

Davies, V. & Cave, R. 1976. Folding and cleavage determined during sedimentation. *Sediment. Geol.* **15**, 89–133.

Dias, R. 1986. Estudo de um sector do autoctone de Tras-os-Montes oriental a ENE, de Torre de Moncorvo. Unpublished M.Sc. thesis, Lisbon University.

Dubey, A. K. & Cobbold, P. R. 1977. Noncylindrical flexural slip folds in nature and experiment. *Tectonophysics* **38**, 223–239.

Duncan, A. C. 1985. Transected folds: a re-evaluation, with examples from the 'type area' at Sulphur Creek, Tasmania. *J. Struct. Geol.* **7**, 409–419.

Elliott, D. 1965. The quantitative mapping of directional minor structures. *J. Geol.* **73**, 865–880.

Evans, A. M. 1963. Conical folding and oblique structures in Charnwood Forest, Leicestershire. *Proc. Yorks. geol. Soc.* **34**, 1, 4, 67–80.

Geiser, P. & Engelder, T. 1983. The distribution of layer parallel shortening fabrics in the Appalachian foreland of New York and Pennsylvania: Evidence for two non-coaxial phases of the Alleghanian orogeny. *Mem. geol. Soc. Am.* **158**, 161–175.

Gray, D. R. 1981. Cleavage–fold relationships and their implications for transected folds: an example from southwest Virginia, U.S.A. *J. Struct. Geol.* **3**, 265–277.

Henderson, J. R., Wright, T. O. and Henderson, M. N. 1986. A history of cleavage and folding: an example from the Goldenville Formation, Nova Scotia. *Bull. geol. Soc. Am.* **97**, 1354–1366.

Hudleston, P. J. 1973. Fold morphology and some geometrical implications of theories of fold development. *Tectonophysics* **16**, 1–46.

James, D. M. D. 1986. The Rhiwnant Inlier, Powys, Mid-Wales. *Geol. Mag.* **123**, 585–587.

Kanagawa, K. 1986. Early Cretaceous folding and cleavage in the Kitakami Mountains, analysed in the Ofanato Terrane. *J. geol. Soc. Japan* **92**, 349–370.

King, S. C. 1987. Structure of the Dingle Peninsula, County Kerry. Unpublished Ph.D. thesis, Queen's University of Belfast.

Lafrance, B. 1989. Structural evolution of a transpression zone in north central Newfoundland. *J. Struct. Geol.* **11**, 705–716.

Mackie, A. H. 1987. The geology of the Llyn Brianna area, Central Wales. Unpublished Ph.D. thesis, University of Cambridge.

Moench, R. H. 1970. Premetamorphic down-to-basin faulting, folding, and tectonic dewatering, Rangeley area, western Maine. *Bull. geol. Soc. Am.* **81**, 1463–1496.

Moseley, F. 1962. The structure of the south-western part of the Sykes Anticline, Bowland, West Yorkshire. *Proc. Yorks. geol. Soc.* **33**, 287–314.

Moseley, F. 1968. Joints and other structures in the Silurian rocks of the southern Shap Fells, Westmorland. *Geol. J.* **6**, 79–96.

Murphy, F. C. 1985. Non-axial planar cleavage and Caledonian sinistral transpression in eastern Ireland. *Geol. J.* **20**, 257–279.

Phillips, W. E. A., Flegg, A. M. & Anderson, T. B. 1979. Strain adjacent to the Iapetus suture in Ireland. In: *The Caledonides of the British Isles—Reviewed* (edited by Harris, A. L., Holland, C. H. & Leake, B. E.). *Spec. Publs geol. Soc. Lond.* **8**, 263–267.

Powell, C. M. 1974. Timing of slaty cleavage during folding of Precambrian rocks, northwest Tasmania. *Bull. geol. Soc. Am.* **85**, 1043–1060.

Price, N. J. 1962. The tectonics of the Aberystwyth Grits. *Geol. Mag.* **94**, 542–557.

Ramsay, J. G. 1963. Structural investigations in the Barberton Mountain Land, Eastern Transvaal. *Trans. geol. Soc. S. Afr.* **66**, 353–401.

Ramsay, J. G. 1967. *Folding and Fracturing of Rocks*. McGraw-Hill, New York.

Ramsay, J. G. & Huber, M. I. 1983. *The Techniques of Modern Structural Geology: Volume 1: Strain Analysis*. Academic Press, London.

Ramsay, J. G. & Huber, M. I. 1987. *The Techniques of Modern Structural Geology, Volume 2: Folds and Fractures*. Academic Press, London.

Roberts, J. L. 1982. *Introduction to Geological Maps and Structures*. Pergamon Press, Oxford.

Sanderson, D. J. 1973. The development of fold axes oblique to the regional trend. *Tectonophysics* **16**, 55–70.

Sanderson, D. J., Andrews, J. R., Phillips, W. E. A. & Hutton, D. H. W. 1980. Deformation studies in the Irish Caledonides. *J. geol. Soc. Lond.* **137**, 289–302.

Sedgwick, A. 1835. Remarks on the structure of large mineral masses. *Trans. geol. Soc.* **2** (ser. 2), 461–486.

Shackleton, R. M. 1958. Downward-facing structures of the Highland Border. *Q. J. geol. Soc. Lond.* **113**, 361–392.

Smith, R. D. A. 1987. Structure and deformation history of the Central Wales Synclinorium, northeast Dyfed: evidence for a long-lived basement lineament. *Geol. J.* **22**, 183–198.

Soper, N. J. 1986. Geometry of anastomosing solution cleavage in transpression zones. *J. Struct. Geol.* **8**, 937–940.

Soper, N. J., Webb, B. C. & Woodcock, N. H. 1987. Late Caledonian (Acadian) transpression in north-west England: timing, geometry and geotectonic significance. *Proc. Yorks. geol. Soc.* **46**, 175–192.

Sorby, H. C. 1853. On the origin of slaty cleavage. *New Phil. J. Edinb.* **55**, 137–148.

Stauffer, M. R. 1963. The geometry of conical folds. New Zealand. *J. geol. Geophys.* **7**, 340–347.

Stauffer, M. R. 1973. New method for mapping fold axial surfaces. *Bull. geol. Soc. Am.* **84**, 2307–2318.

Storey, B. C. & Nell, P. A. R. 1988. Role of strike-slip faulting in the tectonic evolution of the Antarctic Peninsula. *J. geol. Soc. Lond.* **145**, 333–337.

Stringer, P. 1975. Acadian slaty cleavage noncoplanar with fold axial surfaces in the northern Appalachians. *Can. J. Earth Sci.* **12**, 949–961.

Stringer, P. & Treagus, J. E. 1980. Non-axial planar S1 cleavage in the Hawick rocks of the Galloway area, Southern Uplands, Scotland. *J. Struct. Geol.* **2**, 317–331.

Takizawa, F. 1981. Folding structures in the Mesozoic strata of the Ogatsu and Ojika areas, southern Kitakama Mountains—with special reference to slaty cleavage. *Bull. Ass. Struct. Geol. Japan* **26**, 43–57.

Tobisch, O. T. & Paterson, S. C. 1988. Analysis and interpretation of composite foliations in areas of progressive deformation. *J. Struct. Geol.* **10**, 745–754.

Treagus, S. H. 1982. A new isogon-cleavage classification and its application to natural and model fold studies. *Geol. J.* **17**, 49–64.

Treagus, J. E. & Treagus, S. H. 1981. Folds and the strain ellipsoid: a general model. *J. Struct. Geol.* **3**, 1–17.

Twiss, R. J. 1988. Description of folds in single surfaces. *J. Struct. Geol.* **10**, 607–623.

Ward, J. C. 1876. The geology of the northern part of the English Lake District. *Mem. geol. Surv. England and Wales*, **12**.

Whitten, E. H. T. 1966. Sequential multivariable regression methods and scalars in the study of fold geometry variability. *J. Geol.* **74**, 744–763.

Wickham, J. S. 1972. Structural history of a portion of the Blue Ridge, Northern Virginia. *Bull. geol. Soc. Am.* **83**, 723–760.

Wilkinson, I. 1988. The deformation of the Ordovician volcanic rocks of Snowdonia, North Wales. Unpublished Ph.D. thesis, University College of Wales, Aberystwyth.

Williams, P. F. 1985. Multiply deformed terrains—problems of correlation. *J. Struct. Geol.* **7**, 269–280.

Williams, P. F. & Urai, J. L. 1989. Curved vein fibres: an alternative explanation. *Tectonophysics* **158**, 311–333.

Wilson, G. 1967. The geometry of cylindrical and conical folds. *Proc. Geol. Ass.* **78**, 179–209.

Woodcock, N. H. 1976. The accuracy of structural field measurements. *J. Geol.* **84**, 350–355.

Woodcock, N. H. 1977. Specification of fabric shapes using an eigenvalue method. *Bull. geol. Soc. Am.* **88**, 1231–1236.

Woodcock, N. H. 1990. Transpressive Acadian deformation across the Central Wales Lineament. *J. Struct. Geol.* **12**, 329–337.

Woodcock, N. H., Awan, M. A., Johnson, T. E., Mackie, A. H. & Smith, R. D. A. 1988. Acadian tectonics of Wales during Avalonia /Laurentia convergence. *Tectonics* **7**, 483–495.

Woodcock, N. H. and Naylor, M. A. 1983. Randomness testing in three-dimensional orientation data. *J. Struct. Geol.* **5**, 539–548.